

Physics of neutrino flavor transformation through matter-neutrino resonances

Meng-Ru Wu^a, Huaiyu Duan^b, Yong-Zhong Qian^c

^a Institut für Kernphysik (Theoriezentrum), Technische Universität Darmstadt, Schlossgartenstraße 2, 64289 Darmstadt, Germany

^b Department of Physics and Astronomy, University of New Mexico, Albuquerque, NM 87131, USA

^c School of Physics and Astronomy, University of Minnesota, Minneapolis, MN 55455, USA

Abstract

In astrophysical environments such as core-collapse supernovae and neutron star-neutron star or neutron star-black hole mergers where dense neutrino media are present, matter-neutrino resonances (MNRs) can occur when the neutrino propagation potentials due to neutrino-electron and neutrino-neutrino forward scattering nearly cancel each other. We show that neutrino flavor transformation through MNRs can be explained by multiple adiabatic solutions similar to the Mikheyev-Smirnov-Wolfenstein mechanism. We find that for the normal neutrino mass hierarchy, neutrino flavor evolution through MNRs can be sensitive to the shape of neutrino spectra and the adiabaticity of the system, but such sensitivity is absent for the inverted hierarchy.

Keywords: neutrino oscillations, dense neutrino medium, black hole accretion disk, core-collapse supernova

1. Introduction

Neutrino flavor oscillations observed by experiments on solar, atmospheric, reactor and accelerator neutrinos have led to the understanding that neutrinos are massive and their vacuum mass eigenstates are distinct from the weak-interaction states or flavor states, which causes neutrinos to oscillate in vacuum. Remarkable advances have been made in recent years to measure the parameters for neutrino mixing: all the parameters have been measured now except for the neutrino mass hierarchy and the CP-violating phase(s) [1].

When neutrinos propagate through a dense matter, e.g., inside the sun, they can experience a matter potential which stems from the coherent forward scattering by the ordinary matter and leads to the Mikheyev-Smirnov-Wolfenstein (MSW) flavor transformation [2, 3]. In the early universe and near hot, compact objects where dense neutrino media are present, neutrinos can also experience a neutrino potential which arises from the neutrino-neutrino forward scattering or neutrino self-interaction [4–6]. The whole neutrino medium can experience collective oscillations when the neutrino potential dominates (e.g., [7–19]; see also Ref. [20] for a review). There can also be interesting interplay between the matter and neutrino potentials when both are significant [21–27].

Recently, a novel phenomenon of neutrino flavor oscillations, which may occur outside a black-hole accretion disk emitting a larger flux of $\bar{\nu}_e$ than ν_e , was discovered and termed the “matter-neutrino resonance” or MNR [28–30]. This phenomenon can be illustrated by the example of a homogeneous and isotropic neutrino gas which initially consists of mono-energetic ν_e and $\bar{\nu}_e$ only. If initially the antineutrino-neutrino density difference $n_{\bar{\nu}_e} - n_{\nu_e}$ is larger than the electron density n_e and it becomes smaller than n_e later, then the matter and neutrino potentials can (nearly) cancel each other, which results in a resonance [28]. Through MNRs the neutrinos can experience

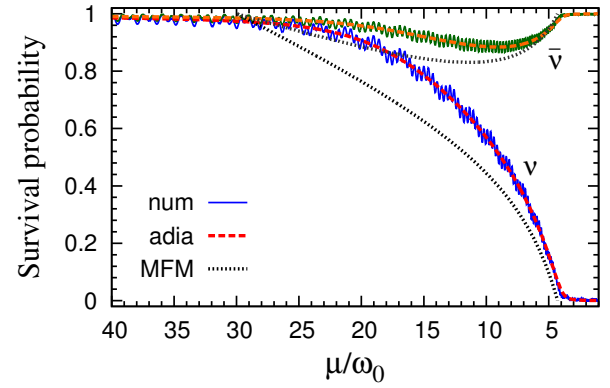


Figure 1: Neutrino survival probabilities as functions of the neutrino-potential strength $\mu = \sqrt{2}G_F n_\nu$ in a slowly expanding, isotropic and homogeneous gas which consists of mono-energetic ν_e and $\bar{\nu}_e$ of vacuum oscillation frequencies $\pm\omega_0$ in the beginning. The solid curves are obtained by solving the flavor-evolution equations numerically (“num”) with $\mu(t) = 100\omega_0 e^{-\omega_0 t/20}$. The dotted curves are obtained by applying the simple MNR criterion proposed by Malkus et al. [28] (“MFM”). The dashed curves represent the fully adiabatic flavor transformation through an MSW-like mechanism (“adia”). All the calculations assume an antineutrino-neutrino ratio $\alpha = n_{\bar{\nu}_e}/n_{\nu_e} = 4/3$, a constant matter potential $\lambda = \sqrt{2}G_F n_e = 10\omega_0$, vacuum mixing angle $\theta_v = 0.15$, and the normal neutrino mass hierarchy.

an almost full flavor conversion in both the normal and inverted (neutrino mass) hierarchies (NH and IH), but the antineutrinos will eventually return to the electron flavor (see Fig. 1). It is intriguing that the simple criterion of the cancellation of the matter and neutrino potentials can be used not only to identify the regime where MNRs occur but also to solve for the flavor evolution of both the neutrino and antineutrino [28]. The physical nature of MNRs, especially why the matter and neutrino potentials should remain nearly equal over a wide range of neutrino densities, is still not completely understood. Similar

phenomena have also been found in core-collapse supernovae when neutrino spin coherence is included [31] or active-sterile neutrino mixing is considered [32].

In this paper we investigate the nature of MNRs. We show that neutrino flavor transformation through MNRs can be explained by an intuitive physical mechanism similar to the standard MSW flavor transformation as first discussed in Ref. [21] and later formulated more explicitly in Ref. [25].

2. Matter-neutrino resonances

2.1. Generalized adiabatic MSW solutions

To elucidate the underlying physics of MNRs, we will again consider the simple example of a homogeneous and isotropic neutrino gas initially consisting of ν_e and $\bar{\nu}_e$ only. As in Ref. [28] we will assume that the neutrino mixing occurs between two active flavors, e and x . We will use the neutrino flavor-isospin (NFIS) \mathbf{s}_ω to represent the flavor quantum state of a neutrino of vacuum oscillation frequency $\omega = \delta m^2/2E$ [24], where $\delta m^2 > 0$ and E are the mass-squared difference and energy of the neutrino, respectively. The NFIS of a neutrino is the expectation value of the flavor-isospin operator $\boldsymbol{\sigma}/2 = \sum_i \mathbf{e}_i \sigma_i/2$ with respect to the (two-component) neutrino flavor wavefunction ψ , where \mathbf{e}_i ($i = 1, 2, 3$) are the orthonormal unit vectors in flavor space, and σ_i are the Pauli matrices. The weak-interaction states $|\nu_e\rangle$ and $|\nu_x\rangle$ are represented by the NFISes in the $+\mathbf{e}_3$ and $-\mathbf{e}_3$ directions, respectively. The vacuum mass eigenstates $|\nu_1\rangle$ and $|\nu_2\rangle$ are represented by the NFISes in the directions of $+\mathbf{B}$ and $-\mathbf{B}$, respectively, where

$$\mathbf{B} = -\mathbf{e}_1 \sin 2\theta_v + \mathbf{e}_3 \cos 2\theta_v. \quad (1)$$

In this paper we will take vacuum mixing angle $\theta_v = 0.15$ and $\pi/2 - 0.15$ for NH and IH, respectively. Also in the NFIS notation the flavor quantum state of an antineutrino is represented by a NFIS of a negative frequency $\omega = -\delta m^2/2E$. A NFIS of a negative ω and in the $+\mathbf{e}_3$ ($-\mathbf{e}_3$) directions represents the weak-interaction state $|\bar{\nu}_x\rangle$ ($|\bar{\nu}_e\rangle$).

The equation of motion of a NFIS \mathbf{s}_ω in a homogeneous, isotropic neutrino gas without collision is [33]

$$\dot{\mathbf{s}}_\omega = \mathbf{s}_\omega \times \mathbf{H}_\omega = \mathbf{s}_\omega \times (\omega \mathbf{B} - \mathbf{V}), \quad (2)$$

where \mathbf{V} represents the neutrino propagation potential in the dense medium.

Neutrino flavor transformation obtains a geometric meaning in the NFIS notation. In vacuum $\mathbf{V} = \mathbf{0}$ and NFIS \mathbf{s}_ω simply precesses about \mathbf{H}_ω with frequency ω . As a result, the probability of the neutrino to be in the electron flavor, which is

$$|\langle \nu_e | \psi \rangle|^2 = \frac{1}{2} + \mathbf{e}_3 \cdot \mathbf{s}_{\omega>0} \quad (3)$$

in the NFIS notation, oscillates with time. This is the vacuum oscillation.

The neutrino propagation potential in an environment of a large matter density but a negligible neutrino density is

$$\mathbf{V} = \lambda \mathbf{e}_3 = \sqrt{2} G_F n_e \mathbf{e}_3, \quad (4)$$

where G_F is the Fermi coupling constant, and n_e is the electron number density. If a ν_e is produced at a high matter density such that $\lambda \gg \omega$ and subsequently the density slowly decreases, then the corresponding NFIS $\mathbf{s}_{\omega>0}$ will stay anti-aligned with \mathbf{H}_ω , which is almost in the $-\mathbf{e}_3$ direction initially and becomes \mathbf{B} when $\lambda \rightarrow 0$. This process describes an adiabatic MSW flavor transformation [34].

When both the matter and neutrino densities are large, the total potential becomes

$$\mathbf{V} = \lambda \mathbf{e}_3 + 2\mu \mathbf{S} = \lambda \mathbf{e}_3 + 2\sqrt{2} G_F n_\nu \mathbf{S}, \quad (5)$$

where n_ν is the total number density of the neutrino, and

$$\mathbf{S} = \int_{-\infty}^{\infty} f_\omega \mathbf{s}_\omega d\omega \quad (6)$$

is the total NFIS. Here we normalize the (constant) neutrino spectrum f_ω with the condition

$$\int_0^\infty f_\omega d\omega = 1. \quad (7)$$

In the spirit of the adiabatic MSW flavor transformation it was proposed in Ref. [25] that, if both the matter and neutrino densities vary slowly and if the NFIS \mathbf{s}_ω initially is aligned (anti-aligned) with the Hamilton vector \mathbf{H}_ω , then the NFIS should keep its alignment (anti-alignment) with \mathbf{H}_ω , i.e.,

$$\mathbf{s}_\omega = \frac{\epsilon_\omega}{2} \frac{\mathbf{H}_\omega}{H_\omega}, \quad (8)$$

where $\epsilon_\omega = +1$ (-1) for the aligned (anti-aligned) configuration. Integrating Eq. (8) one obtains a self-consistent equation

$$\mathbf{S} = \frac{1}{2} \int_{-\infty}^{\infty} \frac{\mathbf{H}_\omega}{H_\omega} \epsilon_\omega f_\omega d\omega, \quad (9)$$

which can be used to solve for the adiabatic solutions. As noted in Ref. [25],

$$\mathbf{s}_\omega \cdot \mathbf{e}_2 = \mathbf{S} \cdot \mathbf{e}_2 = 0 \quad (10)$$

in the adiabatic solution because \mathbf{B} is in the \mathbf{e}_1 - \mathbf{e}_3 plane.

2.2. Monochromatic neutrino gases

As in Ref. [28] we will first consider a neutrino gas consisting of mono-energetic ν_e and $\bar{\nu}_e$ at time $t = 0$ and with the spectrum

$$f_\omega = \alpha \delta(-\omega_0) + \delta(\omega_0), \quad (11)$$

where $\alpha = n_{\bar{\nu}}/n_\nu$ is the ratio of the number density $n_{\bar{\nu}}$ of the antineutrino to the density n_ν of the neutrino. For this system Eq. (2) becomes

$$\dot{\mathbf{s}}_{\pm\omega_0} = \mathbf{s}_{\pm\omega_0} \times \mathbf{H}'_{\pm\omega_0}, \quad (12)$$

where

$$\mathbf{H}'_{\omega_0} = \omega_0 \mathbf{B} - \lambda \mathbf{e}_3 - 2\mu \alpha \mathbf{s}_{-\omega_0}, \quad (13a)$$

$$\mathbf{H}'_{-\omega_0} = -\omega_0 \mathbf{B} - \lambda \mathbf{e}_3 - 2\mu \mathbf{s}_{\omega_0}. \quad (13b)$$

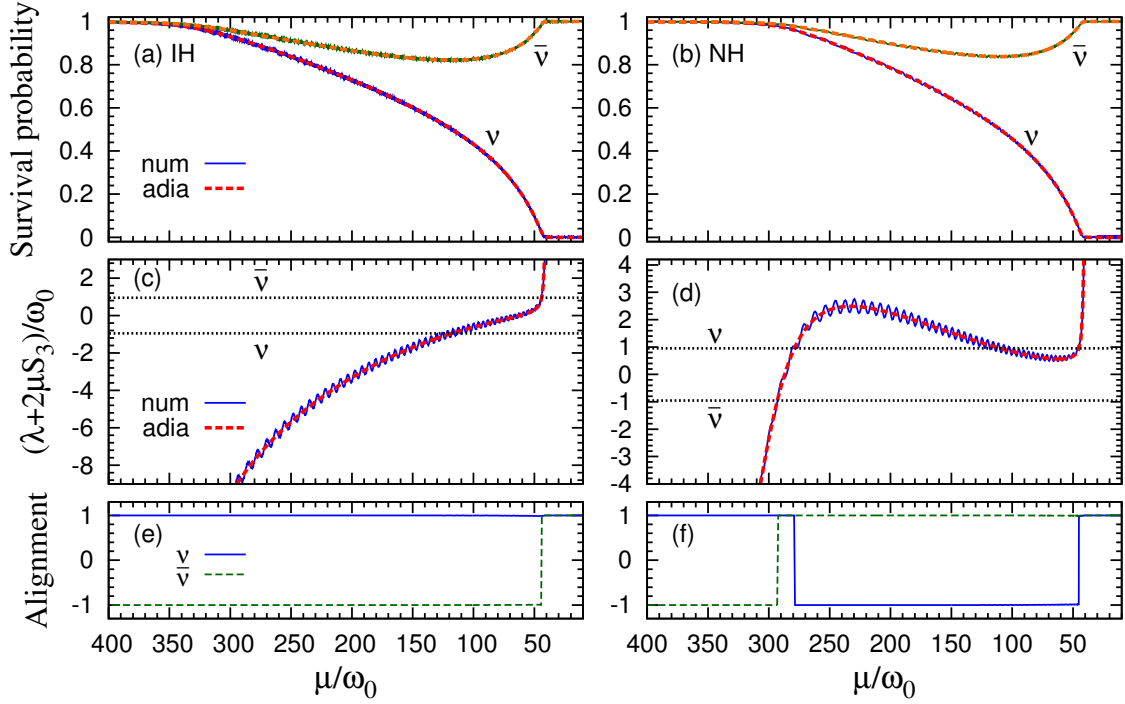


Figure 2: Flavor evolution of a mono-energetic neutrino gas with the inverted (left) and normal (right) neutrino mass hierarchies. Top panels: Neutrino survival probabilities as functions of the strength μ of the neutrino potential for both the numerical (solid) and adiabatic (dashed) solutions. Middle panels: Neutrino propagation potentials $V_3 = \lambda + 2\mu S_3$ as functions of μ . An MSW-like resonance condition is satisfied for the adiabatic solution when the horizontal dotted lines intersect with the dashed curves. Bottoms panels: The alignment factors $\epsilon_{\pm\omega_0}$ of the adiabatic solutions described by Eq. (8) as functions of μ . In all calculations, $\alpha = 4/3$ and $\lambda = 100\omega_0$. Additionally, $\mu = 1000\omega_0 e^{-\omega_0 t/20}$ in the numerical calculations.

Here we have excluded the contributions of $\mathbf{s}_{\pm\omega_0}$ in $\mathbf{H}'_{\pm\omega_0}$ because $\mathbf{s}_\omega \times \mathbf{s}_\omega = \mathbf{0}$. If $\mu > \lambda \gg \omega_0$ at $t = 0$, then $\mathbf{s}_{\pm\omega_0}$ are initially aligned with $\mathbf{H}'_{\pm\omega_0}$, and the adiabatic solution for this system is given by

$$\mathbf{s}_{\pm\omega_0} = \frac{1}{2} \frac{\mathbf{H}'_{\pm\omega_0}}{H'_{\pm\omega_0}}, \quad \mathbf{e}_2 \cdot \mathbf{s}_{\pm\omega_0} = 0. \quad (14)$$

As a first example we look at a monochromatic gas with $\alpha = 4/3$, a constant matter potential $\lambda = 10\omega_0$ and a slowly decreasing neutrino potential $\mu(t) = \mu_0 e^{-t/\tau}$ with $\mu_0 = 100\omega_0$ and $\tau = 20\omega_0^{-1}$. We solved Eq. (12) numerically with NH, and we plot the survival probabilities of the neutrino and the antineutrino in Fig. 1. In the same figure we also plot the results of the adiabatic solution which are in good agreement with the numerical ones. It was proposed in Ref. [28] that the neutrino flavor evolution inside the MNR can be analytically derived if the simple criterion

$$\mathbf{V} \approx \mathbf{0} \quad (15)$$

is applied. We have solved the NFISes as functions of μ which satisfy the above MNR criterion. We shall call this the MFM solution hereafter and plot it in Fig. 1. It is clear from this figure that the adiabatic solution is a more accurate description of the neutrino flavor transformation through MNRs than the MFM solution.

It turns out that the MFM solution is an approximation of the adiabatic solution in the limit $\lambda \gg \omega_0$. To see this we performed another set of calculations as above but with parameters

$\lambda = 100\omega_0$ and $\mu_0 = 1000\omega_0$ for both IH and NH. We plot both the numerical and adiabatic solutions in the upper panels of Fig. 2. In the middle panels of Fig. 2 we plot $V_3 = \lambda + 2\mu S_3$ as functions of μ , which is an indicator of the strength of the total propagation potential \mathbf{V} . Indeed, $|V_3| \ll \lambda$ in the regime where the neutrino experiences flavor conversion. (We have also checked that both $|V_1|$ and $|V_2|$ are small compared to λ throughout the whole process.)

We note that \mathbf{s}_ω represents the flavor quantum state of all neutrinos with the vacuum oscillation frequency ω . A test neutrino represented by \mathbf{s}_ω receives contributions to its propagation potential from other neutrinos also represented by \mathbf{s}_ω but moving in different directions. Therefore, the adiabatic solution should really be described by Eq. (8) with alignment factors $\epsilon_{\pm\omega_0}$. For the antineutrino $\epsilon_{-\omega_0}$ is -1 at $t = 0$ when $\mu > \lambda \gg \omega_0$, and it must become $+1$ sometime later so that the antineutrino returns to the electron flavor when $\mu \rightarrow 0$. In contrast, $\mathbf{s}_{-\omega_0}$ stays aligned with $\mathbf{H}'_{-\omega_0}$ throughout its evolution. To see how this apparent contradiction can be resolved, we introduce the MSW-like resonance condition

$$\omega \cos 2\theta_v - V_3 = \omega \cos 2\theta_v - (\lambda + 2\mu S_3) = 0. \quad (16)$$

In the IH scenario the above resonance condition is satisfied at $\mu/\omega_0 \approx 120$ for the neutrino, which results in a full flavor conversion of the neutrino as expected for adiabatic evolution with $\epsilon_{\omega_0} = +1$. The resonance condition (16) is also satisfied at $\mu/\omega_0 \approx 45$ for the antineutrino. However, because $\mathbf{H}_{-\omega_0}$ actu-

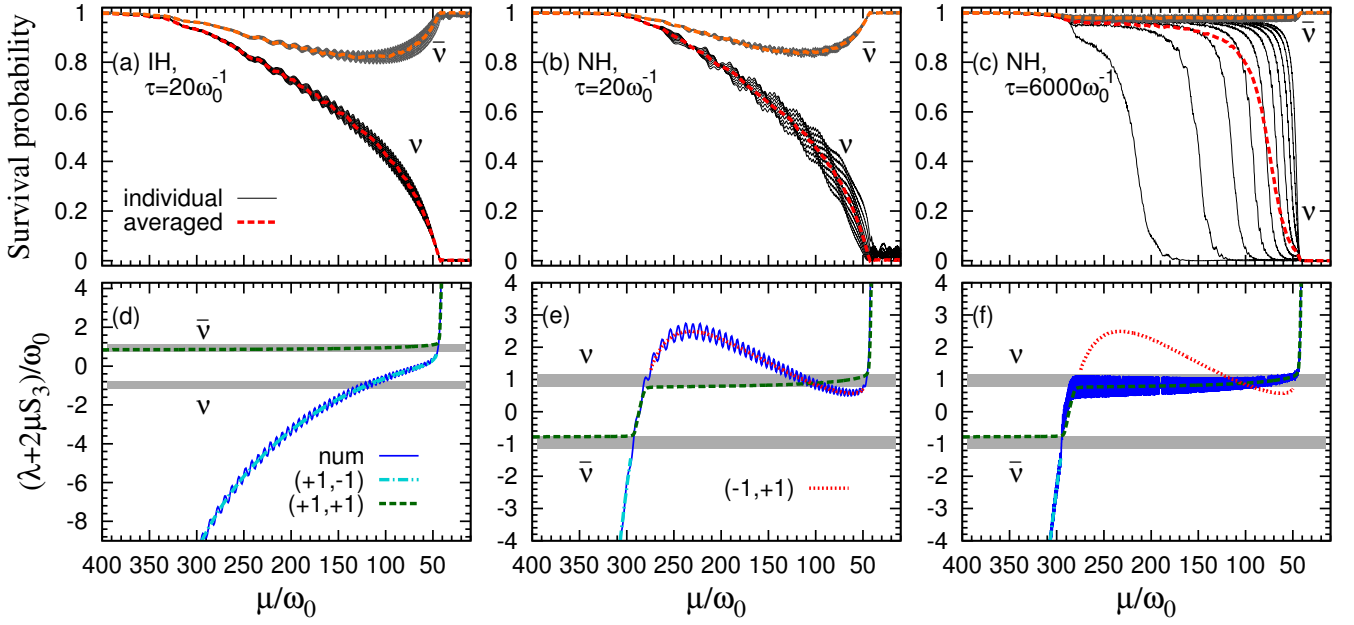


Figure 3: Top panels: Survival probabilities of neutrinos and antineutrinos in a gas which initially consists of pure ν_e and $\bar{\nu}_e$ with the box spectrum described by Eq. (19). The thin solid curves are for individual (anti)neutrinos with $|\omega|/\omega_0 \approx 0.82, 0.86, \dots, 1.18$, and the thick dashed curves are the average survival probabilities. Bottom panels: Neutrino propagation potentials $V_3 = \lambda + 2\mu S_3$ as functions of μ for the numerical solution (solid) and the adiabatic solutions with alignment factors $(\epsilon_v, \epsilon_{\bar{v}}) = (+1, -1)$ (dot-dashed), $(+1, +1)$ (dashed) and $(-1, +1)$ (dotted), respectively. The horizontal bands provide guides to the regions where the MSW-like resonance condition can be satisfied. In all calculations, $\alpha = 4/3$, $\lambda = 100\omega_0$, and $\mu = 1000\omega_0 e^{-t/\tau}$. The neutrino mass hierarchy is inverted for the left panels and normal for the middle and right panels. The expansion time scale is $\tau = 20\omega_0^{-1}$ for the left and middle panels and $6000\omega_0^{-1}$ for the right panels.

ally vanishes at this resonance point, the sudden approximation should apply, i.e., the antineutrino should remain in the same flavor quantum state as that just before the resonance point. As $\mathbf{H}_{-\omega_0}$ grows back in the opposite direction, the alignment factor $\epsilon_{-\omega_0}$ flips sign. In other words, the system has made a “sudden transition” from the solution with alignment configuration $(\epsilon_{\omega_0}, \epsilon_{-\omega_0}) = (+1, -1)$ to that with $(+1, +1)$. This sudden transition between adiabatic solutions with different alignment configurations is the reason why the antineutrino does not change flavor in the end.

The NH scenario is similar but with more twists. In this case the resonance condition (16) is satisfied at $\mu/\omega_0 \approx 280, 110$ and 45 for the neutrino and at $\mu/\omega_0 \approx 290$ for the antineutrino. Only the resonance at $\mu/\omega_0 \approx 110$ produces the full flavor conversion of the neutrino. At the rest of the resonance points the corresponding \mathbf{H}_ω vanishes, which results in sudden transitions between adiabatic solutions with different alignment configurations.

We summarize the evolution of the alignment factors for the adiabatic solutions in both the NH and IH scenarios in the bottom panels of Fig. 2.

2.3. Neutrino gases with box-shape spectra

We now turn to systems with continuous neutrino energy spectra. For such systems we define the antineutrino-neutrino ratio

$$\alpha = \frac{\int_{-\infty}^0 f_\omega d\omega}{\int_0^{\infty} f_\omega d\omega} \quad (17)$$

and the characteristic frequency

$$\omega_0 = \int_0^{\infty} \omega f_\omega d\omega. \quad (18)$$

We first consider a gas which consists of pure ν_e and $\bar{\nu}_e$ in the beginning and with a box-shape spectrum:

$$f_\omega = \begin{cases} 2.5\omega_0^{-1} & \text{if } 0.8\omega_0 \leq \omega \leq 1.2\omega_0, \\ 2.5\alpha\omega_0^{-1} & \text{if } -1.2\omega_0 \leq \omega \leq -0.8\omega_0, \\ 0 & \text{otherwise.} \end{cases} \quad (19)$$

As in the previous example we solved Eq. (2) in the IH scenario with $\alpha = 4/3$, $\lambda = 100\omega_0$, $\mu_0 = 1000\omega_0$ and $\tau = 20\omega_0^{-1}$. We show the survival probabilities of the neutrinos and antineutrinos in Fig. 3(a), which closely resemble the behavior of the monochromatic gas.

Taking hints from the case of the monochromatic gas we also solved for the adiabatic solutions with alignment factors $(\epsilon_v, \epsilon_{\bar{v}}) = (+1, -1)$ and $(+1, +1)$, respectively. Here we have assumed that all neutrinos (antineutrinos) have the same alignment factor ϵ_v ($\epsilon_{\bar{v}}$). We show $V_3(\mu)$ for both the numerical and adiabatic solutions in Fig. 3(d). The comparison between the numerical and adiabatic solutions reveals that, just like the monochromatic gas, the system initially follows the $(+1, -1)$ solution through which the neutrinos experience a flavor conversion because of the resonance at $\mu/\omega_0 \sim 120$. Our calculations suggest that the $(+1, -1)$ solution disappears when it reaches the resonance region for the antineutrinos at $\mu/\omega_0 \sim 45$.

Then the system makes a sudden transition to the $(+1, +1)$ solution as the monochromatic gas does. During this transition the flavor quantum states of the neutrinos and antineutrinos are largely unchanged.

We repeated similar calculations for NH. In the middle and right panels of Fig. 3 we show two typical types of the evolution of the system with $\tau = 20 \omega_0^{-1}$ and $6000 \omega_0^{-1}$, respectively. In both cases the system follows the $(+1, -1)$ solution until it reaches the resonance region of the antineutrino at $\mu/\omega_0 \sim 290$ where the $(+1, -1)$ solution disappears. The system then makes a sudden transition to the $(+1, +1)$ solution until it reaches the first resonance region for the neutrinos at $\mu/\omega_0 \sim 280$. The subsequent evolution of the system depends on the expansion timescale τ .

It is useful to define the adiabaticity parameter for the evolution of a system along a particular adiabatic branch:

$$\gamma_\omega(\tau) = \tau \left| \mathbf{H}_\omega^{\text{adia}} \times \frac{d\mathbf{H}_\omega^{\text{adia}}}{d(\ln \mu)} \right|^{-1} |\mathbf{H}_\omega^{\text{adia}}|^3, \quad (20)$$

where the superscript “adia” indicates a quantity from an adiabatic solution. The larger the value of $\gamma_\omega(\tau)$, the more closely will the system follow the adiabatic solution. As shown in the bottom middle and right panels of Fig. 3, $V_3^{\text{adia}}(\mu)$ of the $(+1, +1)$ solution makes a sharp turn when it reaches the first resonance region for the neutrinos at $\mu/\omega_0 \sim 280$. At this sharp turn $|d\mathbf{H}_\omega^{\text{adia}}/d(\ln \mu)|$ is very large. As a result, the system will continue to follow the $(+1, +1)$ solution only if the evolution is “super-adiabatic” with a large expansion timescale like $\tau = 6000 \omega_0^{-1}$. In this case the neutrinos will experience the flavor conversion in this resonance region. But for a moderate expansion timescale like $\tau = 20 \omega_0^{-1}$, the system will instead make a sudden transition to the $(-1, +1)$ solution as the monochromatic gas does. Then the neutrinos will experience adiabatic flavor conversion when the $(-1, +1)$ solution reaches the second resonance region at $\mu/\omega_0 \sim 110$. Finally the system makes yet another sudden transition back to the $(+1, +1)$ solution when the $(-1, +1)$ solution disappears near the third resonance for the neutrinos at $\mu/\omega_0 \sim 45$.

Although the neutrinos experience flavor conversion in both the monochromatic-like and super-adiabatic types of evolution, there exist important differences between them. In the super-adiabatic evolution $V_3(\mu)$ enters the relevant resonance region from below and stays in this region for a wide range of μ [Fig. 3(f)]. As a result, neutrinos with different energies will pass through the resonance individually, and the high-energy neutrinos will experience flavor conversion first. In the monochromatic-like evolution $V_3(\mu)$ enters the relevant resonance region from above and passes through this region within a narrow range of μ [Fig. 3(d)]. This implies that neutrinos of all energies will go through the resonance almost simultaneously, although the low-energy neutrinos will have flavor conversion slightly earlier than the high-energy ones.

We have explored the flavor evolution of neutrino gases with box spectra of various widths and with different expansion timescales. We found that for the spectrum in Eq. (19) with a width $\Delta\omega = 0.4\omega_0$, the transition from the monochromatic-like

to the super-adiabatic behavior occurs at $\tau \sim 270 \omega_0^{-1}$. As $\Delta\omega$ increases, the resonance region widens so that $V_3^{\text{adia}}(\mu)$ of the $(+1, +1)$ solution makes a less sharp turn when it enters this region, and the transition from the monochromatic-like to the super-adiabatic behavior occurs at a smaller value of τ .

2.4. Neutrino gases with pinched spectra

As more realistic examples we now consider neutrino gases with “pinched” energy spectra of the form $f(E) \propto E^\beta \exp[-(\beta+1)E/\langle E \rangle]$, where β is the pinching parameter and $\langle E \rangle$ is the average neutrino energy [35]. We solved Eq. (2) for the flavor evolution of the neutrino gas with $\beta = 3$ and $\langle E \rangle = 12$ MeV and with various expansion timescales, and the results are plotted in Fig. 4. These results show that the neutrino gases with pinched spectra behave qualitatively similar to those with box spectra. However, because the pinched spectrum we used has a width larger than that of the box spectrum described in Eq. (19), the transition between the monochromatic-like and the super-adiabatic behavior occurs at a much smaller value of τ ($\sim 35 \omega_0^{-1}$). In addition, not all neutrinos and antineutrinos, especially the low-energy ones, will have the same alignment factors as for the systems with a narrow-width box spectrum discussed above. The flavor evolution also becomes non-adiabatic when $\tau \lesssim \omega_0^{-1}$.

3. Conclusions

We have carried out a detailed study of neutrino flavor transformation through MNRs which may occur in astrophysical environments such as core-collapse supernovae and neutron star-neutron star or neutron star-black hole mergers. This interesting phenomenon can potentially impact neutrino-related processes in these environments such as neutrino-driven supernova explosion and neutrino-induced nucleosynthesis. We have shown that the flavor evolution involving MNRs can be explained in terms of adiabatic MSW-like solutions. These solutions are specified by fixed alignment of the flavor isospin of each neutrino (antineutrino) with its Hamiltonian vector. We find that the flavor evolution of the neutrino gases with continuous energy spectra is similar to that of a monochromatic gas if the neutrino mass hierarchy is inverted, and it can exhibit either the monochromatic-like or the super-adiabatic behavior in the normal-hierarchy scenario depending on how slowly the neutrino density decreases.

In our study we have assumed that the neutrino gas was initially dominated by ν_e and $\bar{\nu}_e$ each with a single-peaked spectrum. The behavior of such a system can be modeled by a neutrino gas having a box-shape spectrum with two distinct boxes, each of which is described by a single alignment factor. More complicated phenomena can occur if the neutrino spectra have multiple peaks [14].

As in previous works [28–32] we have assumed that the neutrino gas was homogeneous and isotropic. It is now known that both the homogeneity and isotropy conditions can be broken by collective neutrino oscillations spontaneously [36–44] (see also [45] for a short review). Whether the MNR phenomena can still occur in more realistic settings remains an open

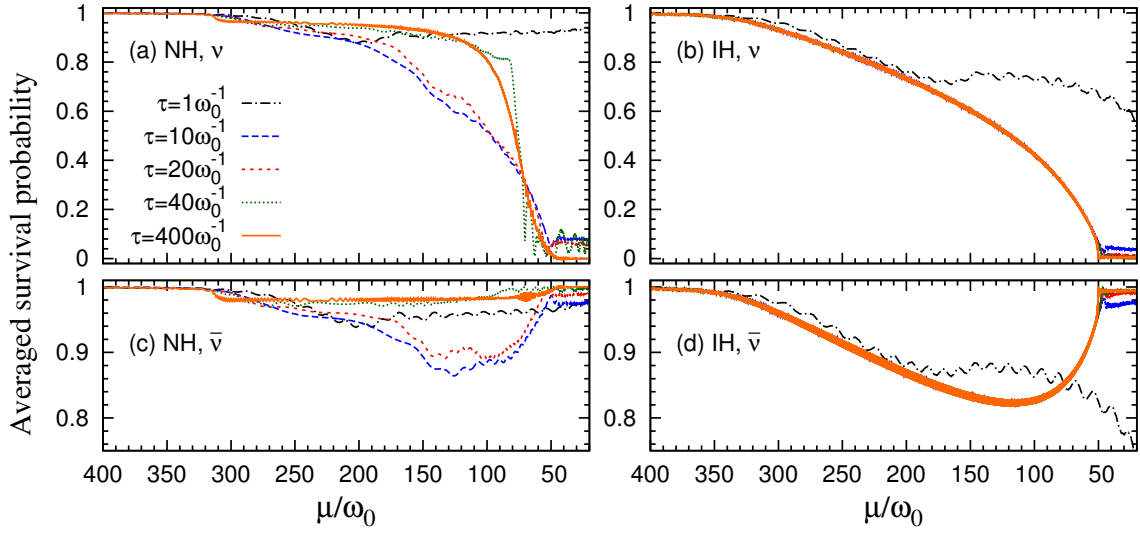


Figure 4: (Color online) Average survival probabilities of neutrinos (top) and antineutrinos (bottom) in a gas with a pinched spectrum ($\beta = 3$ and $\langle E \rangle = 12$ MeV) and with various expansion timescales τ (as labelled) for both the normal (left) and inverted (right) neutrino mass hierarchies. In all calculations, the neutrino mass-squared difference is taken to be $\delta m^2 = 2.44 \times 10^{-3} \text{ eV}^2$, and the rest of the parameters are the same as for Fig. 3.

yet important question, as the ultimate role of neutrinos in associated explosive astrophysical events can only be properly assessed when neutrino flavor transformation in those environments is fully understood.

Acknowledgments

This work was partly supported by the Helmholtz Association (HGF) through the Nuclear Astrophysics Virtual Institute (VH-VI-417) and by the US DOE (EPSCoR grant de-sc0008142 at UNM and grant DE-FG02-87ER40328 at UMN). We thank A. Friedland, G. McLaughlin and D. Vaananen for useful discussions. We also thank the INPAC at Shanghai Jiao Tong University, China for hospitality and support of the Study Group on Neutrino & Nuclear Physics for Nucleosynthesis & Chemical Evolution, which provided the stimulation for this work.

References

- [1] K. A. Olive, et al., Review of Particle Physics, Chin. Phys. C38 (2014) 090001. doi:10.1088/1674-1137/38/9/090001.
- [2] L. Wolfenstein, Neutrino oscillations in matter, Phys. Rev. D17 (1978) 2369.
- [3] S. P. Mikheyev, A. Y. Smirnov, Resonance enhancement of oscillations in matter and solar neutrino spectroscopy, Yad. Fiz. 42 (1985) 1441, [Sov. J. Nucl. Phys. 42, 913 (1985)].
- [4] G. M. Fuller, R. W. Mayle, J. R. Wilson, D. N. Schramm, Resonant neutrino oscillations and stellar collapse, Astrophys. J. 322 (1987) 795.
- [5] D. Notzold, G. Raffelt, Neutrino Dispersion at Finite Temperature and Density, Nucl. Phys. B307 (1988) 924. doi:10.1016/0550-3213(88)90113-7.
- [6] J. T. Pantaleone, Neutrino oscillations at high densities, Phys. Lett. B287 (1992) 128–132. doi:10.1016/0370-2693(92)91887-F.
- [7] V. A. Kostelecký, J. T. Pantaleone, S. Samuel, Neutrino oscillation in the early universe, Phys. Lett. B315 (1993) 46.
- [8] S. Pastor, G. G. Raffelt, D. V. Semikoz, Physics of synchronized neutrino oscillations caused by self-interactions, Phys. Rev. D65 (2002) 053011. arXiv:hep-ph/0109035.
- [9] K. N. Abazajian, J. F. Beacom, N. F. Bell, Stringent constraints on cosmological neutrino antineutrino asymmetries from synchronized flavor transformation, Phys. Rev. D66 (2002) 013008. arXiv:astro-ph/0203442.
- [10] H. Duan, G. M. Fuller, J. Carlson, Y.-Z. Qian, Coherent development of neutrino flavor in the supernova environment, Phys. Rev. Lett. 97 (2006) 241101. arXiv:astro-ph/0608050.
- [11] H. Duan, G. M. Fuller, J. Carlson, Y.-Z. Qian, Simulation of coherent non-linear neutrino flavor transformation in the supernova environment. i: Correlated neutrino trajectories, Phys. Rev. D74 (2006) 105014. arXiv:astro-ph/0606616.
- [12] A. B. Balantekin, Y. Pehlivan, Neutrino-neutrino interactions and flavor mixing in dense matter, J. Phys. G34 (2007) 47. arXiv:astro-ph/0607527.
- [13] G. G. Raffelt, A. Y. Smirnov, Self-induced spectral splits in supernova neutrino fluxes, Phys. Rev. D76 (2007) 081301(R). arXiv:arXiv:0705.1830 [hep-ph].
- [14] B. Dasgupta, A. Dighe, G. G. Raffelt, A. Y. Smirnov, Multiple Spectral Splits of Supernova Neutrinos, Phys. Rev. Lett. 103 (2009) 051105. arXiv:0904.3542, doi:10.1103/PhysRevLett.103.051105.
- [15] A. Friedland, Self-refraction of supernova neutrinos: mixed spectra and three-flavor instabilities, Phys. Rev. Lett. 104 (2010) 191102. arXiv:1001.0996, doi:10.1103/PhysRevLett.104.191102.
- [16] A. Mirizzi, P. D. Serpico, Instability in the Dense Supernova Neutrino Gas with Flavor-Dependent Angular Distributions, Phys. Rev. Lett. 108 (2012) 231102. arXiv:1110.0022, doi:10.1103/PhysRevLett.108.231102.
- [17] A. de Gouvea, S. Shalgar, Effect of transition magnetic moments on collective supernova neutrino oscillations, JCAP 1210 (2012) 027. arXiv:1207.0516, doi:10.1088/1475-7516/2012/10/027.
- [18] J. F. Cherry, J. Carlson, A. Friedland, G. M. Fuller, A. Vlasenko, Neutrino scattering and flavor transformation in supernovae, Phys. Rev. Lett. 108 (2012) 261104. arXiv:1203.1607, doi:10.1103/PhysRevLett.108.261104.
- [19] V. Cirigliano, G. M. Fuller, A. Vlasenko, A New Spin on Neutrino Quantum Kinetics, Phys. Lett. B747 (2015) 27–35. arXiv:1406.5558, doi:10.1016/j.physletb.2015.04.066.
- [20] H. Duan, G. M. Fuller, Y.-Z. Qian, Collective Neutrino Oscillations, Ann. Rev. Nucl. Part. Sci. 60 (2010) 569. arXiv:1001.2799.
- [21] Y. Z. Qian, G. M. Fuller, Neutrino-neutrino scattering and matter enhanced neutrino flavor transformation in supernovae, Phys. Rev. D51 (1995) 1479. arXiv:astro-ph/9406073.
- [22] S. Pastor, G. Raffelt, Flavor oscillations in the supernova hot bubble region: Nonlinear effects of neutrino background, Phys. Rev. Lett. 89

- (2002) 191101. [arXiv:astro-ph/0207281](#).
- [23] A. B. Balantekin, H. Yüksel, Neutrino mixing and nucleosynthesis in core-collapse supernovae, *New J. Phys.* 7 (2005) 51. [arXiv:astro-ph/0411159](#).
 - [24] H. Duan, G. M. Fuller, Y.-Z. Qian, Collective neutrino flavor transformation in supernovae, *Phys. Rev. D* 74 (2006) 123004. [arXiv:astro-ph/0511275](#), doi:10.1103/PhysRevD.74.123004.
 - [25] H. Duan, G. M. Fuller, Y.-Z. Qian, A Simple Picture for Neutrino Flavor Transformation in Supernovae, *Phys. Rev. D* 76 (2007) 085013. [arXiv:0706.4293](#), doi:10.1103/PhysRevD.76.085013.
 - [26] A. Esteban-Pretel, et al., Role of dense matter in collective supernova neutrino transformations, *Phys. Rev. D* 78 (2008) 085012. [arXiv:0807.0659](#), doi:10.1103/PhysRevD.78.085012.
 - [27] J. F. Cherry, M.-R. Wu, J. Carlson, H. Duan, G. M. Fuller, Y.-Z. Qian, Density Fluctuation Effects on Collective Neutrino Oscillations in O-Ne-Mg Core-Collapse Supernovae, *Phys. Rev. D* 84 (2011) 105034. [arXiv:1108.4064](#), doi:10.1103/PhysRevD.84.105034.
 - [28] A. Malkus, A. Friedland, G. C. McLaughlin, Matter-Neutrino Resonance Above Merging Compact Objects [arXiv:1403.5797](#).
 - [29] A. Malkus, J. P. Kneller, G. C. McLaughlin, R. Surman, Neutrino oscillations above black hole accretion disks: disks with electron-flavor emission, *Phys. Rev. D* 86 (2012) 085015. [arXiv:1207.6648](#), doi:10.1103/PhysRevD.86.085015.
 - [30] A. Malkus, G. C. McLaughlin, R. Surman, Symmetric and Standard Matter-Neutrino Resonances Above Merging Compact Objects [arXiv:1507.00946](#).
 - [31] A. Vlasenko, G. M. Fuller, V. Cirigliano, Prospects for Neutrino-Antineutrino Transformation in Astrophysical Environments [arXiv:1406.6724](#).
 - [32] M.-R. Wu, G. Martínez-Pinedo, Y.-Z. Qian, in preparation.
 - [33] G. Sigl, G. Raffelt, General kinetic description of relativistic mixed neutrinos, *Nucl. Phys. B* 406 (1993) 423–451. doi:10.1016/0550-3213(93)90175-0.
 - [34] C. W. Kim, J. Kim, W. K. Sze, On the geometrical representation of neutrino oscillations in vacuum and matter, *Phys. Rev. D* 37 (1988) 1072.
 - [35] M. T. Keil, G. G. Raffelt, H.-T. Janka, Monte Carlo study of supernova neutrino spectra formation, *Astrophys. J.* 590 (2003) 971–991. [arXiv:astro-ph/0208035](#), doi:10.1086/375130.
 - [36] G. Raffelt, S. Sarikas, D. d. S. Seixas, Axial symmetry breaking in self-induced flavor conversion of supernova neutrino fluxes, *Phys. Rev. Lett.* 111 (2013) 091101. [arXiv:1305.7140](#), doi:10.1103/PhysRevLett.111.091101.
 - [37] A. Mirizzi, Multi-azimuthal-angle effects in self-induced supernova neutrino flavor conversions without axial symmetry, *Phys. Rev. D* 88 (7) (2013) 073004. [arXiv:1308.1402](#), doi:10.1103/PhysRevD.88.073004.
 - [38] H. Duan, Flavor Oscillation Modes In Dense Neutrino Media, *Phys. Rev. D* 88 (2013) 125008. [arXiv:1309.7377](#), doi:10.1103/PhysRevD.88.125008.
 - [39] G. Mangano, A. Mirizzi, N. Saviano, Damping the neutrino flavor pendulum by breaking homogeneity, *Phys. Rev. D* 89 (7) (2014) 073017. [arXiv:1403.1892](#), doi:10.1103/PhysRevD.89.073017.
 - [40] H. Duan, S. Shalgar, Flavor instabilities in the neutrino line model, *Phys. Lett. B* 747 (2015) 139–143. [arXiv:1412.7097](#), doi:10.1016/j.physletb.2015.05.057.
 - [41] A. Mirizzi, G. Mangano, N. Saviano, Self-induced flavor instabilities of a dense neutrino stream in a two-dimensional model [arXiv:1503.03485](#).
 - [42] A. Mirizzi, Breaking the symmetries of the bulb model in two-dimensional self-induced supernova neutrino flavor conversions [arXiv:1506.06805](#).
 - [43] S. Chakraborty, R. S. Hansen, I. Izaguirre, G. Raffelt, Self-induced flavor conversion of supernova neutrinos on small scales [arXiv:1507.07569](#).
 - [44] S. Abbar, H. Duan, S. Shalgar, Flavor instabilities in the multi-angle neutrino line model [arXiv:1507.08992](#).
 - [45] H. Duan, Collective neutrino oscillations and spontaneous symmetry breaking, *Int. J. Mod. Phys. E* 24 (2015) 1541008. [arXiv:1506.08629](#), doi:10.1142/S0218301315410086.